IEICE TRANS. ELECTRON., VOL.E96–C, NO.6 JUNE 2013

PAPER Special Section on Analog Circuits and Related SoC Integration Technologies

Two-Tone Signal Generation for ADC Testing

Keisuke KATO[†], **Fumitaka ABE**[†], **Kazuyuki WAKABAYASHI**[†], **Chuan GAO**[†], **Takafumi YAMADA**[†], ***Nonmembers***, **Haruo KOBAYASHI**[†a)], ***Member***, **Osamu KOBAYASHI**[††], ***Nonmember***, ***and*** **Kiichi NIITSU**[†††], ***Member***

SUMMARY This paper describes algorithms for generating low intermodulation-distortion (IMD) two-tone sinewaves, for such as communication application ADC testing, using an arbitrary waveform generator (AWG) or a multi-bit ΣΔ DAC inside an SoC. The nonlinearity of the DAC generates distortion components, and we propose here eight methods to precompensate for the IMD using DSP algorithms and produce low-IMD two-tone signals. Theoretical analysis, simulation, and experimental results all demonstrate the effectiveness of our approach.

key words: *ADC testing, two-tone signal, intermodulation distortion, arbitrary waveform generator, ΣΔ DAC, digital pre-distortion, distortion shaping*

1. Introduction

Two-tone signal testing is frequently used in ADC testing for such as communication applications [1]–[3]. When the third-order nonlinearity is dominant in a signal generator and two frequency components f_1, f_2 ($f_1 \approx f_2$) are used, the third-order intermodulation distortion (IMD3) components $2f_1 - f_2$, $2f_2 - f_1$ are serious because they are close to the signals (i.e., $2f_1 - f_2$, $2f_2 - f_1 \approx f_1$, f_2) and are difficult to remove with an analog filter.

This paper presents eight algorithms to generate low-IMD two-tone signals using a Nyquist-rate DAC or a (multi-bit) ΣΔ DAC followed by an analog filter. Their characteristics are as follows:

1. The proposed methods require just the modification of the digital input for the DAC.
2. Exact identification of the DAC nonlinearity is not required.

Since only a relatively low performance DAC is required for the low-IMD two-tone signal generation, our methods can provide low cost testing of communication application ADCs.

Our methods can reduce the IMD close to f_1, f_2 components but produce spurious components far from f_1, f_2 components which are relatively easy to remove with the following analog filter. We call this as distortion shaping which is similar to but different from noise-shaping in a ΣΔ modulator. Our methods are more effective when the DAC sampling frequency goes higher, because the spurious components goes far away from f_1, f_2 [4]–[10].

Section 2 describes four methods using a Nyquist-rate DAC and Sect. 3 shows the other four methods using a multi-bit ΣΔ DAC. Section 4 provides conclusion.

Manuscript received October 29, 2012.
Manuscript revised January 22, 2013.

[†]The authors are with Division of Electronics and Informatics, Faculty of Science and Technology, Gunma University, Kiryu-shi, 376-8515 Japan.
[††]The author is with Semiconductor Technology Academic Research Center (STARC), Yokohama-shi, 222-0033 Japan.
[†††]The author is with the Department of Electrical Engineering and Computer Science, Graduate School of Engineering, Nagoya University, Nagoya-shi, 464-8603 Japan.
a) E-mail: k_haruo@el.gunma-u.ac.jp

DOI: 10.1587/transele.E96.C.850

2. Low-IMD Two-Tone Signal Generation with Nyquist-Rate DAC

In this section, we consider to generate a low-IMD two-tone signal with a Nyquist-rate DAC inside an SoC, or using an arbitrary waveform generator (AWG) [4], [5], [7], [8], [11] which consists of DSP (or waveform memory) and a Nyquist-rate DAC.

2.1 Proposed Algorithm 1: Phase Switching

We use the following two-signal interleaved input for the DAC (Fig. 1) [4], [5]:

$$D_{in}(n) = \begin{cases} X_1(n) \text{ in case } n\text{:even} \\ X_2(n) \text{ in case } n\text{:odd.} \end{cases} \quad (1)$$

We denote the sampling period of the DAC as T_s and its sampling frequency as f_s (where $T_s f_s = 1$).

We consider the case that third-order distortion is dominant in the DAC and the even harmonic components are small.

$$Y(nT_s) = a_1 D_{in}(n) + a_3 D_{in}(n)^3. \quad (2)$$

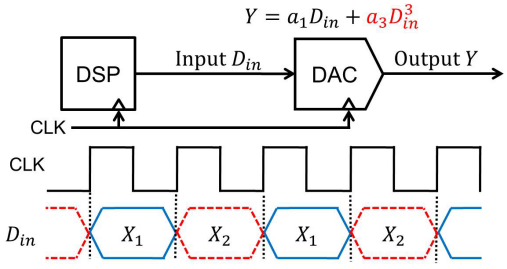

Fig. 1 Proposed method 1, 2 and 3 to generate a low-distortion two-tone signal. DSP provides the input signal X_1 and X_2 alternatively to the following DAC, and distortion components are canceled.

Then we have the following DAC output from Eqs. (1), (2):

$$Y(nT_s) = \begin{cases} a_1X_1(n) + a_3X_1(n)^3 & \text{in case } n\text{:even} \\ a_1X_2(n) + a_3X_2(n)^3 & \text{in case } n\text{:odd.} \end{cases} \quad (3)$$

For a low-IMD3 two-tone signal generation, we propose to use the following:

$$X_1(n) = A\sin\left(2\pi f_1 nT_s + \frac{\pi}{6}\right) + B\sin\left(2\pi f_2 nT_s - \frac{\pi}{6}\right) \quad (4)$$

$$X_2(n) = A\sin\left(2\pi f_1 nT_s - \frac{\pi}{6}\right) + B\sin\left(2\pi f_2 nT_s + \frac{\pi}{6}\right). \quad (5)$$

Then it follows from Eqs. (3), (4) and (5) that

$$\begin{aligned} Y(nT_s) = {} & \frac{\sqrt{3}}{2}\left(a_1A + \frac{a_3}{4}(3A^3 + 6AB^2)\right)\sin(2\pi f_1 nT_s) \\ & + \frac{\sqrt{3}}{2}\left(a_1B + \frac{a_3}{4}(3B^3 + 6A^2B)\right)\sin(2\pi f_2 nT_s) \\ & - \frac{3\sqrt{3}}{8}a_3A^2B\sin(2\pi(2f_1 + f_2)nT_s) \\ & - \frac{3\sqrt{3}}{8}a_3AB^2\sin(2\pi(f_1 + 2f_2)nT_s) \\ & + \frac{1}{2}\left(a_1A + \frac{a_3}{4}(3A^3 + 6AB^2)\right)\cos\left(2\pi\left(\frac{f_s}{2} - f_1\right)nT_s\right) \\ & - \frac{1}{2}\left(a_1B + \frac{a_3}{4}(3B^3 + 6A^2B)\right)\cos\left(2\pi\left(\frac{f_s}{2} - f_2\right)nT_s\right) \\ & - \frac{1}{4}a_3A^3\cos\left(2\pi\left(\frac{f_s}{2} - 3f_1\right)nT_s\right) \\ & + \frac{1}{4}a_3B^3\cos\left(2\pi\left(\frac{f_s}{2} - 3f_2\right)nT_s\right) \\ & - \frac{3}{8}a_3A^2B\cos\left(2\pi\left(\frac{f_s}{2} - 2f_1 - f_2\right)nT_s\right) \\ & + \frac{3}{8}a_3AB^2\cos\left(2\pi\left(\frac{f_s}{2} - f_1 - 2f_2\right)nT_s\right) \\ & + \frac{3}{4}a_3A^2B\cos\left(2\pi\left(\frac{f_s}{2} - 2f_1 + f_2\right)nT_s\right) \\ & - \frac{3}{4}a_3AB^2\cos\left(2\pi\left(\frac{f_s}{2} + f_1 - 2f_2\right)nT_s\right). \end{aligned} \quad (6)$$

We see that the IMD3 ($2f_1 - f_2$, $2f_2 - f_1$) components are canceled in Eq. (6).

Numerical simulation results, shown in Fig. 2, confirm that the IMD3 components are canceled by the proposed algorithm. Since the high-frequency spurious components in Fig. 2 (Right) are far from the signal components f_1, f_2, they are relatively easy to remove by an analog filter after the DAC. Additionally harmonic components have to be removed by the analog filter.

We have performed experiments using an AWG (Agilent 33220A) and a Spectrum Analyzer (ADVANTEST R3267). AWG resolution is 14 bit and sampling rate is 50 MHz. Output frequency is f_1 =200 kHz and f_2 =220 kHz. Figure 3 shows the measurement results and we see that the IMD3 is reduced.

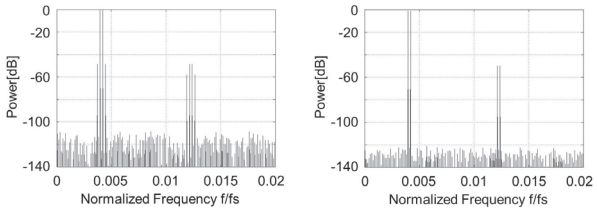

Fig. 2 Simulation results of output power spectrum of a Nyquist-rate DAC with third-order nonlinearity for two-tone input f_1, f_2. (Left) Conventional method. (Right) Proposed method 1.

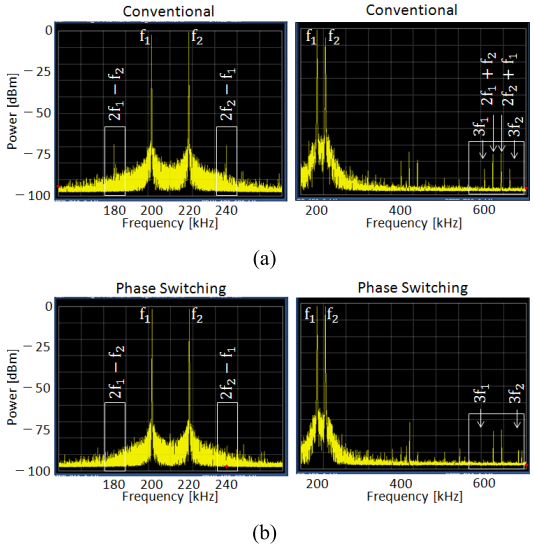

Fig. 3 Experimental results of AWG output power spectrum. (a) Conventional method. (b) Proposed method 1.

Next we consider also fifth-order nonlinearity as follows:

$$Y(nT_s) = a_1D_{in}(n) + a_3D_{in}(n)^3 + a_5D_{in}(n)^5. \quad (7)$$

Then we use the four-phase interleave for the DAC input.

$$D_{in}(n) = \begin{cases} X_1(n) \text{ in case } n = 4k \\ X_2(n) \text{ in case } n = 4k+1 \\ X_3(n) \text{ in case } n = 4k+2 \\ X_4(n) \text{ in case } n = 4k+3. \end{cases} \quad (8)$$

Here k is an integer and

$$\begin{aligned} X_1(n) &= A\sin(2\pi f_1 nT_s + (4/15)\pi) + B\sin(2\pi f_2 nT_s - (4/15)\pi), \\ X_2(n) &= A\sin(2\pi f_1 nT_s + (1/15)\pi) + B\sin(2\pi f_2 nT_s - (1/15)\pi), \\ X_3(n) &= A\sin(2\pi f_1 nT_s - (1/15)\pi) + B\sin(2\pi f_2 nT_s + (1/15)\pi), \\ X_4(n) &= A\sin(2\pi f_1 nT_s - (4/15)\pi) + B\sin(2\pi f_2 nT_s + (4/15)\pi). \end{aligned}$$

Our simulation shows that the IMD3 and IMD5 components are canceled and this is valid even if we change the order of $X_1(n)$, $X_2(n)$, $X_3(n)$ and $X_4(n)$.

The algorithm can be extended to consideration of seventh-order nonlinearity with eight-phase interleave (we have checked by simulation) and so on.

2.2 Proposed Algorithm 2: Frequency Switching

Next we describe the frequency switching algorithm. Let us use the following X_1 and X_2 for the two-phase interleave in Eq. (1):

$$X_1(n) = A\sin(2\pi f_1 nT_s), \quad X_2(n) = B\sin(2\pi f_2 nT_s). \quad (9)$$

Then it follows from Eqs. (3) and (9) that

$$\begin{aligned} Y(nT_s) = {} & \left(\frac{1}{2}a_1A + \frac{3}{8}a_3A^3\right)\sin(2\pi f_1 nT_s) \\ & + \left(\frac{1}{2}a_1B + \frac{3}{8}a_3B^3\right)\sin(2\pi f_2 nT_s) \\ & - \frac{1}{8}a_3A^3\sin(2\pi(3f_1)nT_s) \\ & - \frac{1}{8}a_3B^3\sin(2\pi(3f_2)nT_s) \\ & + \left(\frac{1}{2}a_1A + \frac{3}{8}a_3A^3\right)\cos\left(2\pi\left(\frac{f_s}{2} - f_1\right)nT_s\right) \\ & + \left(\frac{1}{2}a_1B + \frac{3}{8}a_3B^3\right)\cos\left(2\pi\left(\frac{f_s}{2} - f_2\right)nT_s\right) \\ & - \frac{1}{8}a_3A^3\cos\left(2\pi\left(\frac{f_s}{2} - 3f_1\right)nT_s\right) \\ & - \frac{1}{8}a_3B^3\cos\left(2\pi\left(\frac{f_s}{2} - 3f_2\right)nT_s\right). \quad (10) \end{aligned}$$

Our numerical simulations as well as theoretical analysis show that all of the IMD components (such as IMD3, IMD5, IMD7, ...) are canceled (Fig. 4).

Figure 5 shows the measurement results and we see that IMD3 components are reduced.

This algorithm can be extended to the multi-tone signal generation. For example, let us use the following X_1, X_2, X_3 and X_4 for the four-tone signal with the four-phase interleave in Eq. (8):

$$X_1(n) = A_1\sin(2\pi f_1 nT_s), \quad X_2(n) = A_2\sin(2\pi f_2 nT_s),$$
$$X_3(n) = A_3\sin(2\pi f_3 nT_s), \quad X_4(n) = A_4\sin(2\pi f_4 nT_s).$$

Our simulation shows that f_1, f_2, f_3 and f_4 components are generated without IMD components (Fig. 6).

2.3 Proposed Algorithm 3: Combination of Phase and Frequency Switching

Next we describe here an algorithm with combination of phase and frequency switchings, which uses the following four-phase interleave input signal:

$$X_1(n) = A\sin\left(2\pi f_1 nT_s - \frac{\pi}{6}\right), X_2(n) = B\sin\left(2\pi f_2 nT_s + \frac{\pi}{6}\right),$$
$$X_3(n) = A\sin\left(2\pi f_1 nT_s + \frac{\pi}{6}\right), X_4(n) = B\sin\left(2\pi f_2 nT_s - \frac{\pi}{6}\right).$$

This method can cancel HD3 as well as IMD3, and Fig. 7 shows the simulation results. Figure 8 shows the measurement results and we see that IMD3 and HD3 components

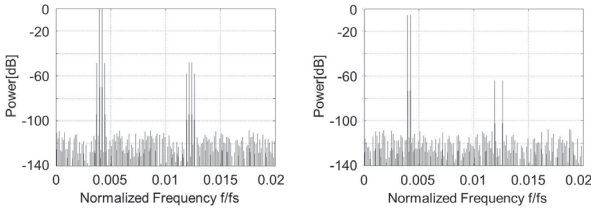

Fig. 4 Simulation results of output power spectrum of a Nyquist-rate DAC with third-order nonlinearity for two-tone input f_1, f_2. (Left) Conventional method. (Right) Proposed method 2.

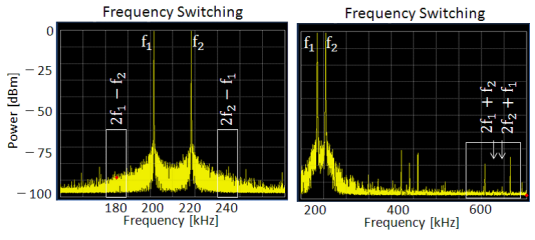

Fig. 5 Experimental results of AWG output power spectrum wih the proposed method 2.

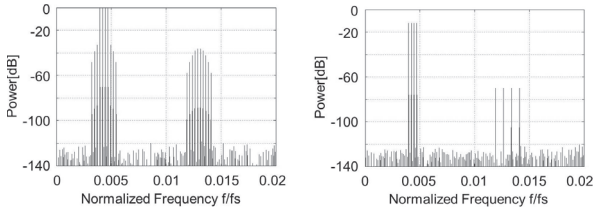

Fig. 6 Simulation results of output power spectrum of a Nyquist-rate DAC with third-order nonlinearity for two-tone input f_1, f_2, f_3 and f_4. (Left) Conventional method. (Right) Proposed method 2.

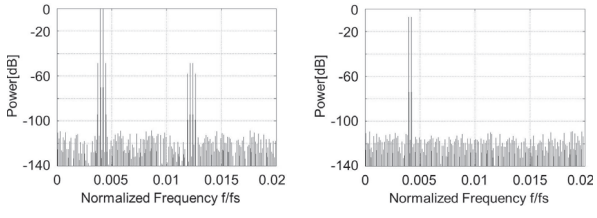

Fig. 7 Simulation results of output power spectrum of a Nyquist-rate DAC with third-order nonlinearity for two-tone input f_1, f_2. (Left) Conventional method. (Right) Proposed method 3.

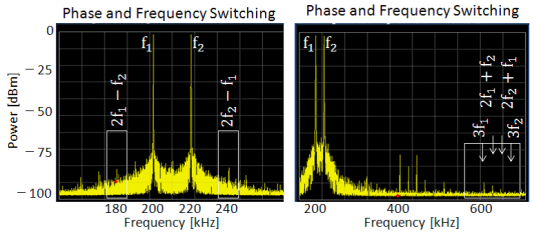

Fig. 8 Experimental results of AWG output power spectrum with the proposed method 3.

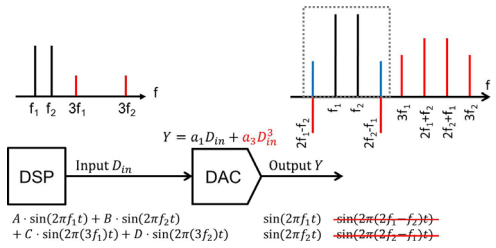

Fig. 9 Principle of the proposed method 4.

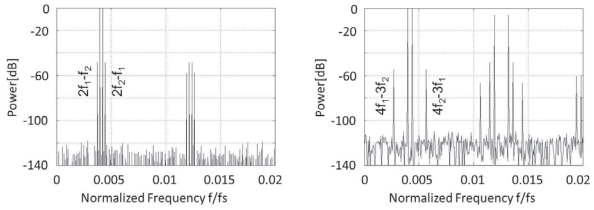

Fig. 10 Simulation results of output power spectrum of a Nyquist-rate DAC with third-order nonlinearity for two-tone input f_1, f_2. (Left) Conventional method. (Right) Proposed method 4.

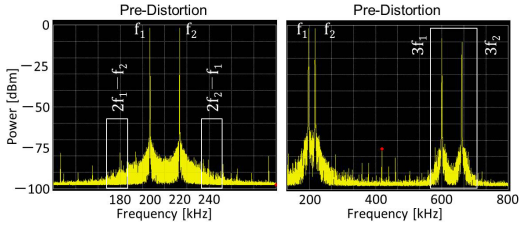

Fig. 11 Experimental results of AWG output power spectrum with the proposed method 4.

are reduced.

2.4 Proposed Algorithm 4: Pre-Distortion

We describe another precompensation method for the IMD3 components using a DSP algorithm by adding $3f_1$, $3f_2$ components at the input (Fig. 9): this concept is similar to the predistortion method in power amplifiers [12].

Suppose that the DAC in the AWG has third-order nonlinearity (Eq. (2)). Then we propose to use the following $D_{in}(n)$:

$$D_{in}(n) = A\sin(2\pi f_1 nT_s) + B\sin(2\pi f_2 nT_s) + C\sin(2\pi(3f_1)nT_s) + D\sin(2\pi(3f_2)nT_s). \quad (11)$$

Here we set

$$C = A/2. \quad D = B/2. \quad (12)$$

By manipulating the above equations (see Appendix), we have V_{out} with f_1, f_2 components and without IMD3 components. V_{out} has other frequency components ($4f_1 - 3f_2$, $4f_2 - 3f_1$) which go far from f_1, f_2 (Figs. 9, 10).

Figure 11 shows the spectrum of the AWG outputs with the conventional and proposed methods. Table 1 shows the effect of proposed methods. Figure 12 shows experimental result comparison of the conventional and proposed methods. We see that IMD3 suppression is substantial with our methods.

We close this section by remarking that $4f_1 - 3f_2$, $4f_2 - 3f_1$ components can be moved to $6f_1 - 5f_2$, $6f_2 - 5f_1$ by adding $5f_1$, $5f_2$ components as well as $3f_1$, $3f_2$ ones at the input, and this can be generalized [8].

Table 1 Experimental result difference of IMD3 suppression between the conventional method and proposed methods 1, 2, 3 & 4.

Proposed Method	IMD3 Suppression [dB]
Phase Switching	11.2
Frequency Switching	10.6
Phase& Frequency Switching	11.3
Pre-Distortion	10.5

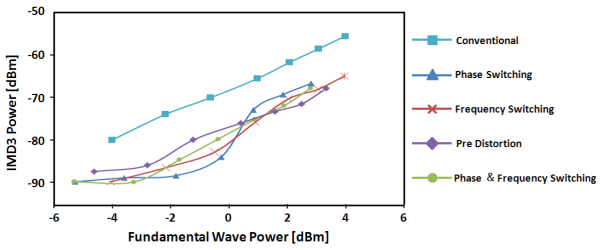

Fig. 12 Experimental result comparison of the conventional, and proposed methods 1, 2, 3 & 4.

3. Proposed Algorithm Using ΣΔDAC

In this section, we consider to generate a low-IMD two-tone signal with a multi-bit ΣΔ DAC. We apply the proposed algorithms 1, 2, 3 and 4 in the Nyquist-rate DAC case to the multi-bit ΣΔ DAC case (Fig. 13) which correspond to the algorithms 5, 6, 7 and 8, respectively. We show with simulations and experiments that all work well, although the analytical proofs may be difficult in ΣΔ DAC case.

Our proposed methods may be implemented by utilizing existing DSP and DAC cores inside an SoC in test mode.

Methods such as dynamic element matching and self-calibration have been used for reducing the effects of multi-bit DAC nonlinearity in ΣΔ modulators [13], but these methods require additional hardware. However, our proposed methods need only a DSP program algorithm change.

3.1 Proposed Algorithm 5: Phase Switching

We apply the proposed algorithm 1 to the multi-bit ΣΔ DAC [6] for low-IMD two-tone signal generation and we use Eqs. (4) and (5). Figure 14 shows simulation results while Fig. 15 shows experimental results for two-tone signal generation (f_1 =1.0 MHz, f_2 =1.1 MHz) using a second-order ΣΔ DAC with 7-bit internal DAC: we see that the proposed

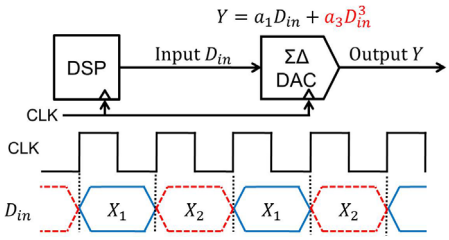

Fig. 13 Proposed methods 5, 6 & 7 to generate a low-distortion two-tone signal with ΣΔ DAC. DSP provides the input signal X_1 and X_2 alternatively to the following ΣΔ DAC, and distortion components are canceled.

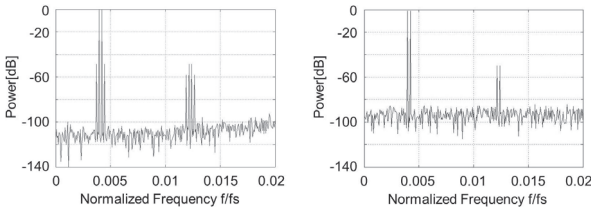

Fig. 14 Simulation results of output power spectrum of a ΣΔ DAC with third-order nonlinearity for two-tone input f_1, f_2. (Left) Conventional method. (Right) Proposed method 5.

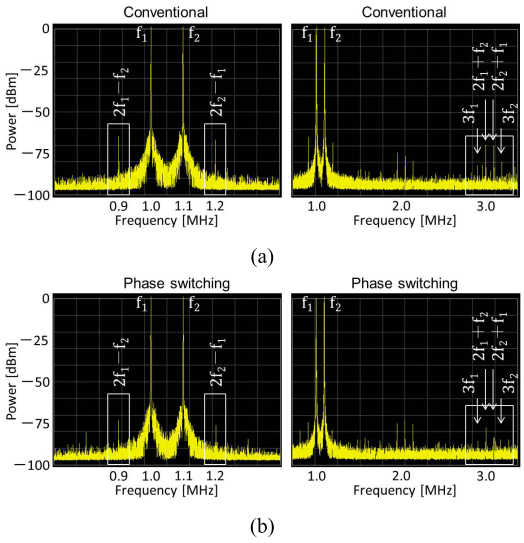

Fig. 15 Experimental results of AWG output power spectrum with a ΣΔ DAC. (a) Conventional method. (b) Proposed method 5.

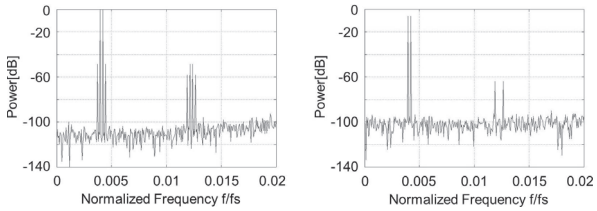

Fig. 16 Simulation results of output power spectrum of a ΣΔ DAC with third-order nonlinearity for two-tone input f_1, f_2. (Left) Conventional method. (Right) Proposed method 6.

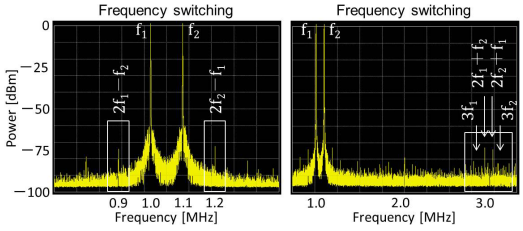

Fig. 17 Experimental results of AWG output power spectrum with a ΣΔ DAC with the proposed method 6.

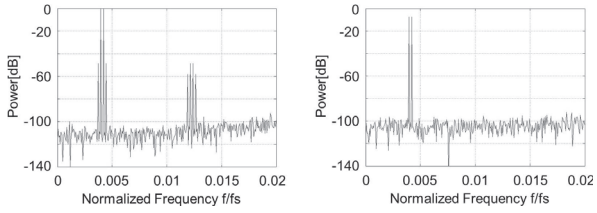

Fig. 18 Simulation results of output power spectrum of a ΣΔ DAC with third-order nonlinearity for two-tone input f_1, f_2. (Left) Conventional method. (Right) Proposed method 7.

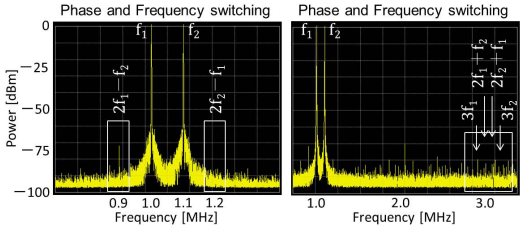

Fig. 19 Experimental results of AWG output power spectrum with a ΣΔ DAC with the proposed method 7.

algorithm reduces IMD3 components.

3.2 Proposed Algorithm 6: Frequency Switching

We apply the proposed algorithm 2 to the multi-bit ΣΔ DAC for low-IMD two-tone signal generation. Figure 16 shows its simulation results while Fig. 17 shows experimental results, and we see that IMD3 components are canceled.

3.3 Proposed Algorithm 7: Combination of Phase and Frequency Switching

We apply the proposed algorithm 3 to the multi-bit ΣΔ DAC for low-IMD two-tone signal generation. Figure 18 shows its simulation results while Fig. 19 shows experimental results, and we see that IMD3 and HD3 components are canceled.

3.4 Proposed Algorithm 8: Pre-Distortion

We apply the proposed algorithm 4 to the multi-bit ΣΔ DAC for low-IMD two-tone signal generation (Fig. 20). Figure 21 shows its simulation results while Fig. 22 shows experimental results. We see that IMD3 components go away from the signals f_1, f_2.

Table 2 shows the effect of proposed methods. Fig-

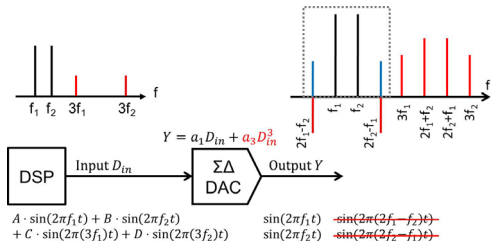

Fig. 20 Principle of the proposed method 8.

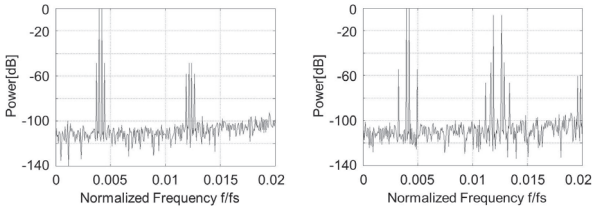

Fig. 21 Simulation results of output power spectrum of a ΣΔ DAC with third-order nonlinearity for two-tone input f_1, f_2. (Left) Conventional method. (Right) Proposed method 8.

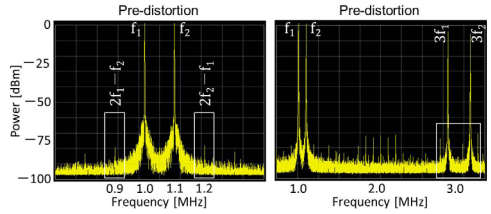

Fig. 22 Experimental results of AWG output power spectrum with a ΣΔ DAC with the proposed method 8.

Table 2 Experimental result difference of IMD3 suppression between the conventional method and proposed methods 5, 6, 7 & 8.

Proposed Methods	IMD3 Suppression [dB]
Phase Switching	6.47
Frequency Switching	6.83
Phase& Frequency Switching	5.96
Pre-Distortion	9.30

ure 23 shows experimental result comparison of the conventional and proposed methods. We see that IMD3 suppression is substantial with our methods.

4. Concluding Remarks

We have proposed eight algorithms for generating low-IMD two-tone sinewaves, for testing communication application ADCs, using an arbitrary waveform generator (AWG) or a multi-bit ΣΔ DAC inside an SoC. Theoretical analysis, simulation, and experimental results verified the effectiveness of our approach.

The proposed methods can be used in the loopback test inside a communication SoC [14] as well as in AWG signal

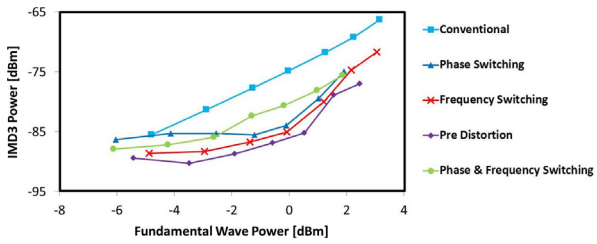

Fig. 23 Experimental result comparison of the conventional, and proposed methods 5, 6, 7 & 8.

Table 3 Output power spectrum comparison.

	Cancel	Appear
Conventional		$2f_1 - f_2, 2f_2 - f_1$
Phase Switching	$2f_1 - f_2, 2f_2 - f_1$ $3f_1, 3f_2$	around $f_s/2$
Frequency Switching	$2f_1 - f_2, 2f_2 - f_1$ $2f_1 + f_2, 2f_2 + f_1$	around $f_s/2$
Phase& Frequency Switching	$2f_1 - f_2, 2f_2 - f_1$ $2f_1 + f_2, 2f_2 + f_1$ $3f_1, 3f_2$	around $f_s/4$, $f_s/2$
Pre-Distortion	$2f_1 - f_2, 2f_2 - f_1$ $3f_1 - 2f_2, 3f_2 - 2f_1$	$4f_1 - 3f_2, 4f_2 - 3f_1$ around $3f_1, 5f_1, 7f_1, 9f_1$

generation; we utilize DACs and DSP cores inside the SoC and generate ADC testing signals in test mode.

All of our methods do not need the DAC nonlinearity identification, and we need only DSP program (or waveform memory contents) change. Our methods become more effective as the DAC frequency goes high, but do not require the DAC linearity, which meets the semiconductor device advancement trends.

All of our methods can be interpreted as injecting high frequency components as the DAC input to cancel IMD3 components caused by the DAC nonlinearity.

Table 3 shows the comparison of the conventional and proposed methods when the third-order nonlinearity is dominant: there, "cancel" means the canceled spurious or harmonic components and "appear" means the spurious components caused by the corresponding method. Further investigation for merits and demerits of each algorithm, in the view points of signal frequency, IMD reduction, analog filter requirements [15] and DAC sampling speed & resolution is underway.

We have the following observation based on our theoretical analysis as well as simulation and experimental results:

- The phase switching and frequency switching methods would be comparably effective when the DAC has only the third-order nonlinearity, because both methods cause spurious tones around $f_s/2$ and cannot cancel $2f_1 + f_2$, $2f_2 + f_1$ (in phase switching case) or $3f_1$, $3f_2$ (in frequency switching case).
- Theoretically, the frequency switching method can cancel all of the intermodulation distortion components even if the DAC has, say, the fifth-order nonlinearity.
- According to our experiments, the phase switching is

slightly better for the reduction of $2f_1 - f_2$, $2f_2 - f_1$ components, though this may depend on experimental conditions.

- The phase & frequency switching method can cancel $2f_1 + f_2$, $2f_2 + f_1$, $3f_1$, $3f_2$ but cause relatively large spurious components around $f_s/4$. This method will be more effective as the sampling frequency f_s increases, because the spurious components around $f_s/4$ goes far away from f_1, f_2.
- The pre-distortion method remain the spurious components relatively close to f_1, f_2 but the high frequency spurious components around $f_s/2$ are much smaller compared to the other methods. This method may be useful in applications where the high frequency spurious components are very harmful.

Finally we remark that the proposed techniques in this paper are to apply for conventional DACs, however we have also exploited a new DAC architecture in [16] to reduce the IMD3 components for the two-tone signal generation for next generation AWGs.

Acknowledgment

We acknowledge Y. Yano, T. Gake, N. Takai, T. Matsuura, T. J. Yamaguchi, H. Miyashita, K. Rikino, S. Kishigami, H. Okawara, H. Sakayori and K. Wilkinson.

References

[1] Y. Motoki, H. Sugawara, H. Kobayashi, T. Komuro, and H. Sakayori, "Multi-tone curve fitting algorithms for communication application ADC testing," Electronics and Communication in Japan: Part 2, vol.86, no.8, pp.1–11, 2003.
[2] M. Gustavsson, J.J. Wikner, and N.N. Tan, CMOS Data Converters for Communications, Kluwer Academic Publisher, 2000.
[3] B. Razavi, RF Microelectronics, Prentice Hall, 1998.
[4] K. Wakabayashi, T. Yamada, S. Uemori, O. Kobayashi, K. Kato, H. Kobayashi, K. Niitsu, H. Miyashita, S. Kishigami, K. Rikino, Y. Yano, and T. Gake, "Low-distortion single-tone and two-tone sinewave generation algorithms using an arbitrary waveform generator," IEEE International Mixed-Signals, Sensors and Systems Test Workshop, Santa Barbara, CA, May 2011.
[5] K. Wakabayashi, K. Kato, T. Yamada, O. Kobayashi, H. Kobayashi, F. Abe, and K. Niitsu, "Low-distortion sinewave generation method using arbitrary waveform generator," J. Electronic Testing: Theory and Applications, Special Issue on Analog, Mixed-Signal, RF and MEMS Testing, vol.28, no.5, pp.641–651, Oct. 2012.
[6] T. Yamada, O. Kobayashi, K. Kato, K. Wakabayashi, H. Kobayashi, T. Matsuura, Y. Yano, T. Gake, K. Niitsu, N. Takai, and T.J. Yamaguchi, "Low-distortion single-tone and two-tone sinewave generation using ΣΔ DAC," IEEE International Test Conference (poster session), Anaheim, CA, Sept. 2011.
[7] K. Kato, F. Abe, K. Wakabayashi, T. Yamada, H. Kobayashi, O. Kobayashi, and K. Niitsu "Low-IMD two-tone signal generation for ADC testing," IEEE International Mixed-Signals, Sensors, and Systems Test Workshop, Taipei, Taiwan, May 2012.
[8] K. Kato, K. Wakabayashi, T. Yamada, H. Kobayashi, O. Kobayashi, and K. Niitsu, "Low-distortion two-tone signal generation with AWG," IEICE Workshop on Circuits and Systems, Awaji-Shima, Japan, Aug. 2012.
[9] K. Kato, F. Abe, K. Wakabayashi, C. Gao, T. Yamada, H. Kobayashi, O. Kobayashi, and K. Niitsu, "Two-tone signal generation for communication application ADC testing," 21st IEEE Asian Test Symposium, Niigata, Japan, Nov. 2012.
[10] K. Kato, M. Murakami, F. Abe, Y. Arai, H. Kobayashi, T. Matsuura, S. Mohyar, K, Ramin, O. Kobayashi, K. Niitsu, and N. Takai, "Low-cost high-quality signal generation for ADC testing," IEEE International Test Conference, (Special Poster Session), Anaheim, CA, Nov. 2012.
[11] A. Maeda, "A method to generate a very low distortion, high frequency sine waveform using an AWG," IEEE International Test Conference, Santa Clara, CA, Oct. 2008.
[12] S.C. Cripps, Advanced Techniques in RF Power Amplifier Design, pp.153–195, Artec House, 2002.
[13] R. Schreier and G.C. Temes, Understand Delta-Sigma Data Converters, IEEE Press, 2005.
[14] M. Laisne, "Future challenges for mixed signal SOC testing," IEEE International Mixed-Signals, Sensors and Systems Test Workshop, Santa Barbara, CA, May 2011.
[15] F. Abe, K. Kato, H. Kobayashi, O, Kobayashi, N. Takai, and K. Niitsu, "Analog filter for low-distortion sinewave generation using arbitrary waveform generator" IEEJ Technical Meeting of Electronic Circuits, ECT-12-075, Kumamoto, Japan, May 2012.
[16] C. Gao, K. Wakabayashi, K. Kato, F. Abe, H. Kobayashi, O. Kobayashi, T. Matsuura, K. Niitsu, and N. Takai, "Digital-to-analog converter architecture for low distortion signal generation," IEEJ Technical Meeting of Electronic Circuits, ECT-12-20, Yokosuka, Japan, March 2012.

Appendix

This appendix shows that the IMD3 components $2f_1 - f_2$, $2f_2 - f_1$ go away from f_1, f_2 using the proposed algorithm 4. We assume the third-order nonlinearity (Eq. (2)) in the DAC.

$$y(t) = \alpha x(t) + \beta x(t)^3.$$

We use the following input $x(t)$ in the algorithm 4:

$$\begin{aligned} x(t) &= A\sin(\omega_1 t) + B\sin(\omega_2 t) \\ &\quad + C\sin(3\omega_1 t) + D\sin(3\omega_2 t). \end{aligned}$$

Here $\omega_1 = 2\pi f_1$ and $\omega_2 = 2\pi f_2$. Then we have the following output $y(t)$:

$$\begin{aligned} y(t) &= \left\{\alpha A + \frac{1}{4}\beta\left(3A^3 + 6AB^2 + 6AC^2 + 6AD^2 - 3A^2C\right)\right\} \\ &\quad \times \sin(\omega_1 t) \\ &+ \left\{\alpha B + \frac{1}{4}\beta\left(3B^3 + 6A^2B + 6BC^2 + 6BD^2 - 3B^2D\right)\right\} \\ &\quad \times \sin(\omega_2 t) \\ &+ \left\{\alpha C + \frac{1}{4}\beta\left(3C^3 + 6A^2C + 6B^2C + 6CD^2\right)\right\}\sin(3\omega_1 t) \\ &+ \left\{\alpha D + \frac{1}{4}\beta\left(3D^3 + 6A^2D + 6B^2D + 6C^2D\right)\right\}\sin(3\omega_2 t) \\ &+ \beta/4 \cdot \{\left(-3A^2C + 3AC^2\right)\sin(5\omega_1 t) \\ &\quad + \left(-3B^2D + 3BD^2\right)\sin(5\omega_2 t)\} \\ &- 3\beta/4 \cdot \left(AC^2\sin 7\omega_1 t + BD^2\sin 7\omega_2 t\right) \\ &- \beta/4 \cdot \left(C^3\sin 9\omega_1 t + D^3\sin 9\omega_2 t\right) \\ &+ \beta/4 \cdot \left(-3A^2B + 6ABC\right) \end{aligned}$$

$$
\begin{aligned}
&\times \{\sin(2\omega_1+\omega_2)t - \sin(2\omega_1-\omega_2)t\} \\
+\ &\beta/4\cdot\left(-3AB^2+6ABD\right) \\
&\times \{\sin(\omega_1+2\omega_2)t + \sin(\omega_1-2\omega_2)t\} \\
+\ &\beta/4\cdot\left(-3B^2C+6BCD\right) \\
&\times \{\sin(3\omega_1+2\omega_2)t + \sin(3\omega_1-2\omega_2)t\} \\
+\ &\beta/4\cdot\left(-3A^2D+6ACD\right) \\
&\times \{\sin(2\omega_1+3\omega_2)t - \sin(2\omega_1-3\omega_2)t\} \\
-\ &3\beta/2\cdot ABC\{\sin(4\omega_1+\omega_2)t - \sin(4\omega_1-\omega_2)t\} \\
-\ &3\beta/2\cdot ABD\{\sin(\omega_1+4\omega_2)t + \sin(\omega_1-4\omega_2)t\} \\
-\ &3\beta/2\cdot ACD\{\sin(4\omega_1+3\omega_2)t - \sin(4\omega_1-3\omega_2)t\} \\
-\ &3\beta/2\cdot BCD\{\sin(3\omega_1+4\omega_2)t + \sin(3\omega_1-4\omega_2)t\} \\
-\ &3\beta/4\cdot BC^2\{\sin(6\omega_1+\omega_2)t - \sin(6\omega_1-\omega_2)t\} \\
-\ &3\beta/4\cdot AD^2\{\sin(\omega_1+6\omega_2)t + \sin(\omega_1-6\omega_2)t\} \\
-\ &3\beta/4\cdot C^2D\{\sin(6\omega_1+3\omega_2)t - \sin(6\omega_1-3\omega_2)t\} \\
-\ &3\beta/4\cdot CD^2\{\sin(3\omega_1+6\omega_2)t + \sin(3\omega_1-6\omega_2)t\}.
\end{aligned}
$$

We see that in case $C = A/2$, $D = B/2$, then $2f_1-f_2$, $2f_2-f_1$, $3f_1-2f_2$ and $3f_2-2f_1$ components are canceled.

Keisuke Kato received the B.S. and M.S. degrees in electronic engineering from Gunma University in 2011 and 2013 respectively, and he is currently working for Mitsubishi Electric Corporation. His research interests include ADC testing technology.

Fumitaka Abe received the B.S. degree (honored) in electronic engineering from Gunma University in 2012 and he is currently a master course student there. His research interests lie in ADC testing technology.

Kazuyuki Wakabayashi received the B.S. degree from Tokyo University of Technology in 2009 and the M.S. degree in electronic engineering from Gunma University in 2011. He is currently working for Fujitsu Ltd. where he is engaged in firmware design for optical transceivers. His research interests include ADC testing technology, power supply and power amplifier circuits.

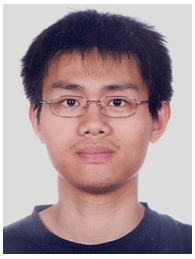

Chuan Gao received the B.S. degree in telecommunication and information engineering from Nanjing University of Posts and Telecommunications (NUPT), China in 2010, and the M.S. degree in electronic engineering from Gunma University, Japan in 2013. Currently he is working for ALPS ELECTRIC CO., LTD. His research interests lie in digital control of power supply circuitry and mixed-signal SoC test technology.

Takafumi Yamada received the B.S. and M.S. degrees in electronic engineering from Gunma University in 2009 and 2011 respectively. He is currently working for Nippon Signal Co., Ltd. His research interests include sigma-delta AD/DA modulator design and ADC testing technology.

Haruo Kobayashi received the B.S. and M.S. degrees in information physics from University of Tokyo in 1980 and 1982 respectively, the M.S. degree in electrical engineering from University of California at Los Angeles (UCLA) in 1989, and the Ph.D. degree in electrical engineering from Waseda University in 1995. He joined Yokogawa Electric Corp. Tokyo, Japan in 1982, and was engaged in research and development related to measuring instruments. In 1997, he joined Gunma University and presently is a Professor in division of electronics and informatics there. His research interests include mixed-signal integrated circuit design & testing, and signal processing algorithms.

Osamu Kobayashi received the B.S. and M.S. degrees in electric and electronic engineering from Tokyo Institute of Technology in 1982 and 1984 respectively. He joined Fujitsu Ltd. Kanagawa, Japan in 1984, and was engaged in developing analog IPs for CMOS Mixed Signal LSI. From 2007 to 2009, he joined Fujitsu Laboratories LTD. He is currently working for Semiconductor Technology Academic Research Center.

Kiichi Niitsu was born in Japan, in 1983. He received the B.S. degree summa cum laude, M.S. and Ph.D. degrees in electrical engineering from Keio University, Yokohama, Japan, in 2006, 2008 and 2010, respectively. From 2010 to 2012, he was an Assistant Professor at Gunma University, Kiryu, Japan. He is currently a Lecturer at Nagoya University, Nagoya, Japan. From April 2013 to September 2013, he has been with the Centre for Bio-Inspired Technology in Imperial College London, United Kingdom as a visiting researcher. His current research interest lies in the low-power and high-speed VLSI design for biomedical application. From 2008 to 2010, Dr. Niitsu was a Research Fellow of the Japan Society for the Promotion of Science (JSPS), a Research Assistant of the Global Center of Excellence (GCOE) Program at Keio University and a Collaboration Researcher of the Keio Advanced Research Center (KARC). He received the 2007 INOSE Science Promotion Award from the Foundation of Electrical, Electronics, and Information Science Promotion, the 2008 IEEE SSCS Japan Chapter Young Researcher Award and the 2009 IEEE SSCS Japan Chapter Academic Research Award both from IEEE Solid-State Circuits Society Japan Chapter. In 2011, he was awarded YASUJIRO NIWA OUTSTANDING PAPER AWARD, FUNAI Research Promotion Award, Ando Incentive Prize for the Study of Electronics, and Ericsson Young Scientist Award.